Compound-Specific Chlorine Isotope Fractionation in Biodegradation of Atrazine†

Christina Lihl[a,b], Benjamin Heckel[a,b], Anna Grzybkowska[c], Agnieszka Dybala-Defratyka[c], Violaine Ponsin[d,e] , Clara Torrentó[d,f], Daniel Hunkeler[d], Martin Elsner[a,b,*]

[a] Institute of Groundwater Ecology, Helmholtz Zentrum München, Ingolstädter Landstraße 1, 85764 Neuherberg, Germany

[b] Chair of Analytical Chemistry and Water Chemistry, Technical University of Munich, Marchioninistraße 17, 81377 Munich, Germany

[c] Institute of Applied Radiation Chemistry, Faculty of Chemistry, Lodz University of Technology, Zeromskiego 116, 90-924 Lodz, Poland

[d] Centre of Hydrogeology and Geothermics (CHYN), University of Neuchâtel, 2000 Neuchâtel, Switzerland

[e] Département des sciences de la Terre et de l'atmosphère, Université du Québec à Montréal, 201 avenue du Président Kennedy, Montréal, QC, Canada

[f] Grup MAiMA, Departament de Mineralogia, Petrologia i Geologia Aplicada, Facultat de Ciències de la Terra, Universitat de Barcelona (UB), C/ Martí i Franquès s/n, 08028, Barcelona, Spain.

* Corresponding Author: Phone: +49 89/2180-78231. E-mail: m.elsner@tum.de

† Electronic Supplementary Information (ESI) available: Information concerning the HPLC temperature programs, two Figures and one Table illustrating the GC-qMS method optimization for chlorine analysis, one Table illustrating the method comparison of the GC-qMS for chlorine analysis, one Figure and one Table considering H-abstraction during chlorine CSIA, two Figures illustrating the results of HPLC concentration analysis.

KEYWORDS: hydrolysis, oxidative dealkylation, compound-specific isotope analysis, chlorine isotope effect, Arthrobacter, Rhodococcus

Graphical Abstract:

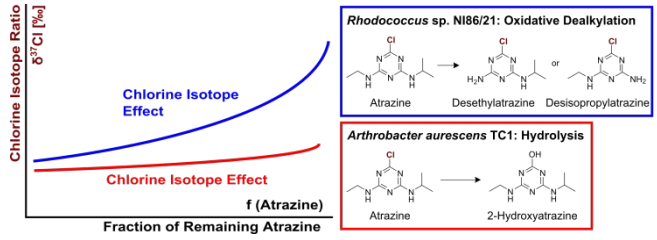

Environmental Significance:

Atrazine is an important chlorinated micropollutant. Although degradable *via* different pathways (dealkylation and hydrolytic dechlorination), it is often recalcitrant and persists in groundwater. To assess and understand its degradation pathways, compound-specific carbon and nitrogen isotope analysis has been advanced, but information from chlorine isotope fractionation has been missing until today. This study explores the added benefit of chlorine isotope fractionation as indicator of natural atrazine transformation. Together with carbon and nitrogen isotope analysis, this enables a multi-element approach which can improve source identification and differentiation of microbial transformation pathways in the environment.

ABSTRACT

Atrazine is a frequently detected groundwater contaminant. It can be microbially degraded by oxidative dealkylation or by hydrolytic dechlorination. Compound-specific isotope analysis is a powerful tool to assess its transformation. In previous work, carbon and nitrogen isotope effects were found to reflect these different transformation pathways. However, chlorine isotope fractionation could be a particularly sensitive indicator of natural transformation since chlorine isotope effects are fully represented in the molecular average while carbon and nitrogen isotope effects are diluted by non-reacting atoms.

Therefore, this study explored chlorine isotope effects during atrazine hydrolysis with *Arthrobacter aurescens* TC1 and oxidative dealkylation with *Rhodococcus* sp. NI86/21. Dual element isotope slopes of chlorine vs. carbon isotope fractionation ($\Lambda^{Arthro}_{Cl/C}$ = 1.7 ± 0.9 vs. $\Lambda^{Rhodo}_{Cl/C}$ = 0.6 ± 0.1) and chlorine vs. nitrogen isotope fractionation ($\Lambda^{Arthro}_{Cl/N}$ = -1.2 ± 0.7 vs. $\Lambda^{Rhodo}_{Cl/N}$ = 0.4 ± 0.2) provided reliable indicators of different pathways. Observed chlorine isotope effects in oxidative dealkylation (ε_{Cl} = -4.3 ± 1.8 ‰) were surprisingly large, whereas in hydrolysis (ε_{Cl} = -1.4 ± 0.6 ‰) they were small, indicating that C-Cl bond cleavage was not the rate-determining step. This demonstrates the importance of constraining expected isotope effects of new elements before using the approach in the field. Overall, the triple element isotope information brought forward here enables a more reliable identification of atrazine sources and degradation pathways.

INTRODUCTION

The herbicide atrazine has been used in agriculture to inhibit growth of broadleaf and grassy weeds[1]. In the U.S. atrazine was the second most commonly used herbicide in 2012 and is still in use today[2]. In the European Union atrazine was banned in 2004[3], but together with its metabolites it is still frequently detected at high concentrations in groundwater[4, 5]. The massive and widespread use has led to a wide-ranging presence of atrazine in the environment, which can have harmful effects on living organisms and humans[6]. Therefore, the environmental fate of atrazine is of significant concern and much attention has been directed at detecting and enhancing its natural biodegradation. However, assessing microbial degradation of atrazine in the environment is challenging with conventional methods like concentration analysis. Sorption and remobilization of the parent compound and its metabolites, as well as further transformation of the metabolites inevitably lead to fluctuations in concentrations[7-10], which make it difficult to assess the net extent of atrazine degradation in the field.

In recent years, compound-specific isotope analysis (CSIA) has been proposed as an alternative approach to detect and quantify the degradation of atrazine[11-13].

In contrast to, and complementary to traditional methods, CSIA informs about transformation without the need to detect metabolites. The reason is that during (bio)chemical transformations molecules with heavy isotopes are typically enriched in the remaining substrate since their bonds are more stable and, therefore, usually react slower

than molecules containing light isotopes (normal kinetic isotope effect). The ratios of heavy to light isotopes (e.g. $^{13}C/^{12}C$ for carbon) in the remaining substrate, therefore, change during transformation. Observing such changes can be used as direct (and concentration-independent) indicator of degradation[14, 15].

Isotope values are reported in the δ-notation relative to an international reference material, e.g. for carbon[14, 15]:

$$\delta^{13}C = [(^{13}C/^{12}C)_{Sample} - (^{13}C/^{12}C)_{Reference}] / (^{13}C/^{12}C)_{Reference} \quad (1)$$

The magnitude of the degradation-induced isotope fractionation depends on different factors, which can make isotope ratios of specific elements particularly attractive to observe degradation-induced isotope fractionation. To this end, first, an element needs to be directly involved in the (bio)chemical reaction. For example, a carbon isotope effect would be quite generally expected in organic molecules, whereas a chlorine isotope effect would be primarily expected if a C-Cl bond is cleaved. Second, isotope fractionation depends on the underlying kinetic isotope effect (see above), but also on the extent to which this effect is represented in the molecular average isotope fractionation described by the enrichment factor ε (see below). Atrazine, for example, contains only one chlorine atom but eight carbon and five nitrogen atoms. Hence, chlorine isotope effects at the reacting position are fully represented in the molecular average, whereas position-specific carbon and nitrogen isotope effects are diluted by non-reacting atoms[14, 15].

Most of the publications studying the chemical mechanisms of abiotic and microbial atrazine degradation have focused on the analysis of carbon ($^{13}C/^{12}C$) and nitrogen ($^{15}N/^{14}N$) isotope fractionation. Thereby, ε-values in the range of -5.4 ‰ to -1.8 ‰ for carbon and -1.9 ‰ to 3.3 ‰ for nitrogen were observed[9, 10, 16, 17]. Chlorine isotope effects for microbial atrazine degradation were so far not reported due to analytical challenges[18]: Until recently[19, 20], suitable methods were not available for chlorine isotope analysis of atrazine. However, from the magnitude of chlorine isotope effects observed for dechlorination of trichloroethenes (-5.7 ‰ to -3.3 ‰, where intrinsic isotope effects are diluted by a factor of three[21]), very large chlorine enrichment factors ε_{Cl} (-8 ‰ to -10 ‰ or even larger) could potentially occur for a C-Cl bond cleavage in atrazine. For example, enzymatic hydrolysis of the structural homologue ametryn (atrazine structure with a -SCH_3 instead of a -Cl group) yielded a sulfur isotope enrichment factor ε_S of -14.7 ‰ ± 1.0 ‰[17]. If the cleavage of carbon-chlorine bonds is involved in the rate-determining step of a (bio)transformation, chlorine isotope effects could, therefore, enable a particularly sensitive detection of natural transformation processes by compound-specific (i.e., molecular average) isotope analysis.

The measurement of chlorine isotope fractionation is attractive for yet another reason – multiple element isotope analysis bears potential for a better distinction of sources and transformation pathways. From isotope analysis of one element alone, it is difficult to distinguish sources of a particular compound, or competing transformation pathways that

may lead to metabolites of different toxicity[15]. For example, two different microbial transformation pathways can lead to the degradation of atrazine in the environment. Hydrolysis forms the nontoxic dehalogenated product 2-hydroxyatrazine (HAT) whereas oxidative dealkylation degrades atrazine to the still herbicidal products desethyl- (DEA) or desisopropylatrazine (DIA)[22, 23]. Prominent examples for microorganisms catalyzing these pathways are *Arthrobacter aurescens* TC1 and *Rhodococcus* sp. NI86/21 (see Figure 1). *A. aurescens* TC1 was directly isolated from an atrazine-contaminated soil[24]. By expressing the enzyme TrzN, it is capable of performing hydrolysis of atrazine[24, 25]. *Rhodococcus* sp. NI86/21 uses a cytochrome P450 system for catalyzing oxidative dealkylation of atrazine[26].

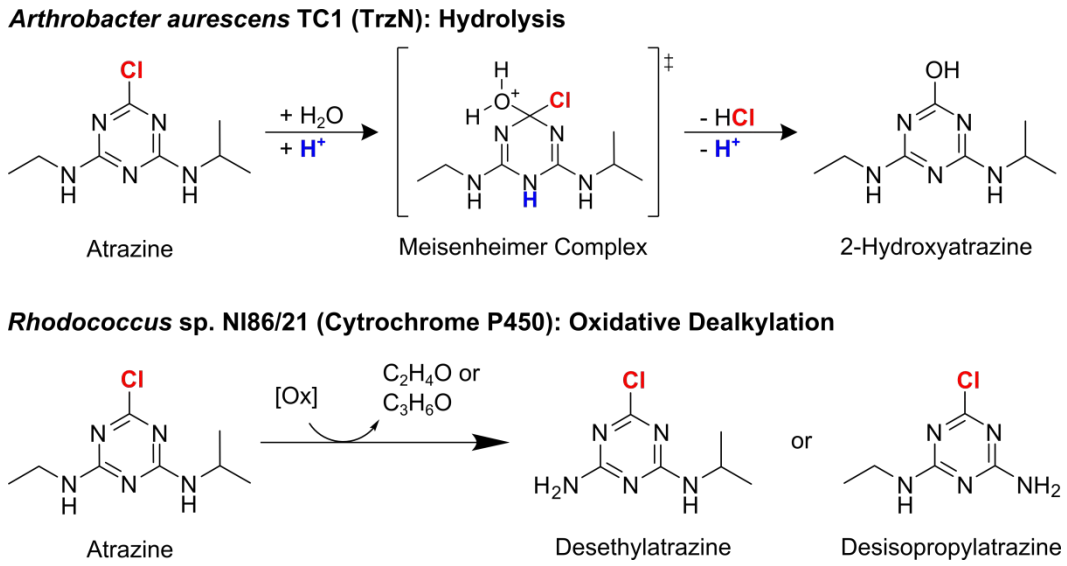

Figure 1. Microbial degradation of atrazine by *Arthrobacter aurescens* TC1 and *Rhodococcus* sp. NI86/21 (adapted from Meyer et al.[9] and Meyer & Elsner[10]).

For these two pathways, carbon isotope fractionation was very similar, but significant differences were observed in nitrogen isotope effects[9, 10, 16, 17]. Plotting the changes of isotope ratios of these two elements relative to each other results in the regression slope Λ for carbon and nitrogen[27, 28]

$$\Lambda_{C/N} = \Delta\delta^{15}N / \Delta\delta^{13}C \approx \varepsilon_N / \varepsilon_C \quad (2)$$

Hence, dual element (C, N) isotope trends for oxidative dealkylation of atrazine with *Rhodococcus* sp. NI86/21 ($\Lambda^{Rhodo}_{C/N}$ = 0.4 ± 0.1)[16] were significantly different compared to hydrolysis with *A. aurescens* TC1 ($\Lambda^{Arthro}_{C/N}$ = -0.6 ± 0.1)[9] offering an opportunity to distinguish atrazine degradation pathways in the field. However, in environmental assessments it is advantageous to have isotopic information of as many elements as possible in order to distinguish degradation pathways and sources at the same time[29-31]. Therefore, information from a third element, chlorine, would be highly valuable. Also on the mechanistic end, information gained from a change in the chlorine isotope value could lead to a more reliable differentiation of transformation pathways and contribute to a better mechanistic understanding of the underlying chemical reaction[31]. Along these lines, triple element (3D) isotope analysis was already accomplished for chlorinated alkanes[31, 32] and alkenes[33, 34].

Until now, however, compound-specific chlorine isotope analysis has not been accessible so that chlorine isotope ratio changes for hydrolysis of atrazine have only been analyzed in abiotic systems or via computational calculations[35, 36]. For oxidative

dealkylation, chlorine isotope effects have, so far, not been studied. Recently a GC-qMS method for chlorine isotope analysis of atrazine has been brought forward[20] which offers the opportunity to enable deeper mechanistic insights into its transformation processes. Therefore, our objective was to analyze carbon, nitrogen and chlorine isotope effects associated with the biodegradation of atrazine via hydrolysis with *A. aurescens* TC1 and via oxidative dealkylation with *Rhodococcus* sp. NI86/21. In addition, we computationally predicted the chlorine isotope effect associated with hydrolysis and oxidative dealkylation for comparison. Further, we evaluated whether the additional information from chlorine isotope fractionation is a particularly sensitive indicator for transformation processes and whether it can confirm previously proposed mechanisms of different pathways. With this study, we bring forward information about degradation-induced chlorine isotope fractionation of atrazine as a basis to apply triple element (3D) isotope analysis in environmental assessments.

MATERIAL & METHODS

Bacterial strains and cultivation. *A. aurescens* strain TC1 was grown in mineral salt medium supplemented with approx. 20 mg/L of atrazine according to the protocol of Meyer et al.[9] Likewise, *Rhodococcus* sp. strain NI86/21 was cultivated in autoclaved nutrient broth (8 g/L, Difco™) with approx. 20 mg/L of atrazine according to the protocol of Meyer et al.[16]. In the late-exponential growth phase the strains were harvested via centrifugation (4000 rpm, 15 min). For the start of the degradation experiments, cell

pellets of each strain were transferred to 400 mL fresh media and atrazine was added to achieve a starting concentration of 20 mg/L. All experiments were performed in triplicate at 21 °C on a shaker at 150 rpm. Control experiments, which were performed without the bacterial strains, did not show any degradation of atrazine.

Concentration measurements via HPLC. The process of atrazine degradation was monitored by concentration measurements. For analysis, 1 mL samples were taken and filtered through a 0.22 µm filter. Atrazine and its degradation products were directly analyzed using a Shimadzu UHPLC-20A system, which was equipped with an ODS column 30 (Ultracarb 5 µM, 150 × 4.6 mm, Phenomenex). After sample injection (10 µL) an adequate gradient program (see SI) was used for compound separation. The oven temperature was set to 45 °C and the compounds were detected by their UV absorbance at 222 nm. Quantitation was performed by the software “Lab Solutions” based on internal calibration curves.

Preparation of samples for isotope analysis. According to the protocol of Meyer et al.[9] between 10 and 260 mL of sample were taken for isotope analysis of atrazine at every sampling event. After centrifugation (15 min, 4000 rpm) the supernatant was collected in a new vial. Subsequently, samples were extracted by adding dichloromethane (5-130 mL) and shaking the vial for at least 20 min. The sample extracts were dried at room temperature under the fume hood. Afterwards, the dried extracts were dissolved in ethyl acetate to a final atrazine concentration of approx. 200 mg/L.

Isotope analysis of carbon and nitrogen. The protocol for isotope analysis of carbon and nitrogen was adapted from the studies of Meyer et al.[9, 16]. A TRACE GC Ultra gas chromatograph hyphenated with a GC-III combustion interface and coupled to a Finnigan MAT253 isotope ratio mass spectrometer (GC-C-IRMS, all Thermo Fisher Scientific) was used. Each sample was analyzed in triplicate. Sample injection (2-3 µL) was performed by a Combi-PAL autosampler (CTC Analysis). The injector had a constant temperature of 220 °C, was equipped with an "A" type packed liner for large volume injections (GL Sciences) and was operated for 1 min in splitless and then in split mode (split ratio 1:10) with a flow rate of 1.4 mL/min. For peak separation, the GC oven was equipped with a DB-5 MS column (30 m × 0.25 mm, 1 µm film thickness, Agilent). The temperature program of the oven started at 65 °C (held for 1 min), ramped at 20 °C/min to 180 °C (held for 10 min) and ramped again at 15 °C/min to 230 °C (held for 8 min). In the combustion interface, a GC Isolink II reactor (Thermo Fisher Scientific) was installed, which was operated at a temperature of 1000 °C. After combustion of the analytes to CO_2 and subsequent reduction of any nitrogen oxides, the compounds were analyzed as CO_2 for carbon and N_2 for nitrogen isotope measurements. Three pulse of CO_2 or N_2, respectively, were introduced at the beginning and at the end of each run as monitoring gas. Beforehand, these monitoring gases were calibrated against RM8563 (CO_2) and NSVEC (N_2), which were supplied by the International Atomic Energy Agency (IAEA). The analytical uncertainty 2σ was ±0.5 ‰ for carbon isotope values and ±1.0 ‰ for nitrogen isotope values.

Isotope analysis of chlorine. For chlorine isotope analysis of atrazine, a 7890A gas chromatograph coupled to a 5975C quadrupole mass spectrometer (GC-qMS, both Agilent) was used. Sample injection (2 µL) was performed by a PaI Combi-xt autosampler (CTC Analysis). For the injector and the GC oven, the same parameters as for carbon and nitrogen isotope analysis were used with the exception that a different liner type, a "FocusLiner" (SGE), was used. The ion source had a constant temperature of 230 °C and the quadrupole of 150 °C. Prior to sample analysis, the method of Ponsin et al.[20] was tested and optimized for our instrument (see details in SI). Chlorine isotope ratios were evaluated by monitoring the mass-to-charge ratio m/z of 202/200. Standards and samples were measured ten times each and uncertainties were reported as standard deviation. Results were only evaluated if the peak areas of samples were inside a defined linearity range (peak area of 1.2×10^8 – 3.0×10^8 for m/z 200). Inside the linearity range, the determined precision of the method is associated with a maximal deviation of ±1.1 ‰. For analysis, the samples were diluted with ethyl acetate to a final concentration of approx. 75 mg/L and measured with a dwell time of 100 ms. Correction of the chlorine isotope values relative to Standard Mean Ocean Chloride (SMOC) was performed by an external two-point calibration with characterized standards of atrazine (Atr #4 $\delta^{37}Cl$ = -0.89 ‰ and Atr #11 $\delta^{37}Cl$ = +3.59 ‰)[37]. To this end, the standards were measured at the beginning, in between and at the end of each sequence.

Evaluation of stable isotope fractionation. Determination of isotope enrichment factors ε was achieved by the Rayleigh equation, which describes the gradual enrichment of the residual substrate fraction ƒ with molecules containing heavy isotopes, as expressed by isotope values according to eq. 1[15, 38]. For example, for chlorine:

$$\ln [(\delta^{37}Cl + 1) / (\delta^{37}Cl_0 + 1)] = \varepsilon_{Cl} \bullet \ln f \quad (3)$$

Here $\delta^{37}Cl_0$ refers to the chlorine isotope value at the starting point (t = 0) of an experiment. Regression slopes Λ of dual element isotope plots were obtained by plotting isotope ratios of two different elements against each other, e.g. carbon vs. nitrogen (see eq. 2). The uncertainties of the calculated ε-values and Λ-values are reported as 95 % confidence intervals (CI). Furthermore, (apparent) kinetic isotope values, $(A)KIE_{Cl}$, that express the ratio of reaction rates ^{35}k and ^{37}k of heavy and light isotopologues, respectively,

$$KIE_{Cl} = {}^{35}k / {}^{37}k \quad (4)$$

were calculated according to Elsner et al.[15] by converting ε_{Cl}-values into $(A)KIE_{Cl}$ and taking into account that atrazine contains only one chlorine atom (n = 1):

$$(A)KIE_{Cl} = 1 / (n \times \varepsilon_{Cl} + 1) \quad (5)$$

Prediction of chlorine kinetic isotope effects during oxidative dealkylation and hydrolysis of atrazine. In the computational part of the study, we considered hydrogen atom transfer and hydride transfer taking place at the α-position of the ethyl side chain of the atrazine

molecule in the oxidative dealkylation reaction promoted by permanganate and the hydronium ion, respectively. Furthermore, we considered hydrolysis under acidic/enzymatic, neutral and alkaline conditions. All molecular structures and analytical vibrational frequencies for involved reactant complexes and transition states were taken from a previous study[16]. Chlorine kinetic isotope effects on dealkylation were calculated using the complete Bigeleisen equation[39] implemented in the ISOEFF program[40] at 300 K. Additional isotope effects predictions for hydrolysis under acidic as well as neutral conditions were performed following the previous computational protocol[36]. The tunneling contributions to the overall kinetic isotope effect were omitted.

RESULTS & DISCUSSION

Observation of normal chlorine isotope effects in biotic hydrolysis and oxidative dealkylation. Atrazine degradation by *A. aurescens* TC1 resulted in the metabolite 2-hydroxyatrazine, whereas the metabolites DEA and DIA were observed for *Rhodococcus* sp. NI86/21 (see Figure S4 and S5 in the SI). Detection of these expected degradation products (Figure 1) demonstrates that hydrolysis and oxidative dealkylation were the underlying biochemical reactions during atrazine degradation, respectively. In both biodegradation experiments – biotic hydrolysis with *A. aurescens* TC1 and oxidative dealkylation with *Rhodococcus* sp. NI86/21 – normal chlorine isotope fractionation was observed (see Figure 2A). In the three replicates of hydrolytic degradation by *A. aurescens* TC1 90 %, 90 % and 60 % transformation of atrazine was reached after

approx. 26 h, respectively (see SI, Figure S4). Evaluation of $\delta^{37}Cl$ values during biotic hydrolysis according to Equation 3 resulted in a small normal isotope effect of ε_{Cl} = -1.4 ± 0.6 ‰. In oxidative dealkylation with *Rhodococcus* sp. NI86/21 approx. 90 % degradation was reached after approx. 186 h in all three replicates (see SI, Figure S5). Evaluation of changes in chlorine isotope ratios resulted in a surprisingly large normal isotope effect of ε_{Cl} = -4.3 ± 1.8 ‰ considering that the C-Cl bond is not broken during the reaction (see Figure 1). In a next step, carbon and nitrogen isotope effects were therefore analyzed to confirm whether the same reactions mechanisms are at work as observed in previous studies[9, 16].

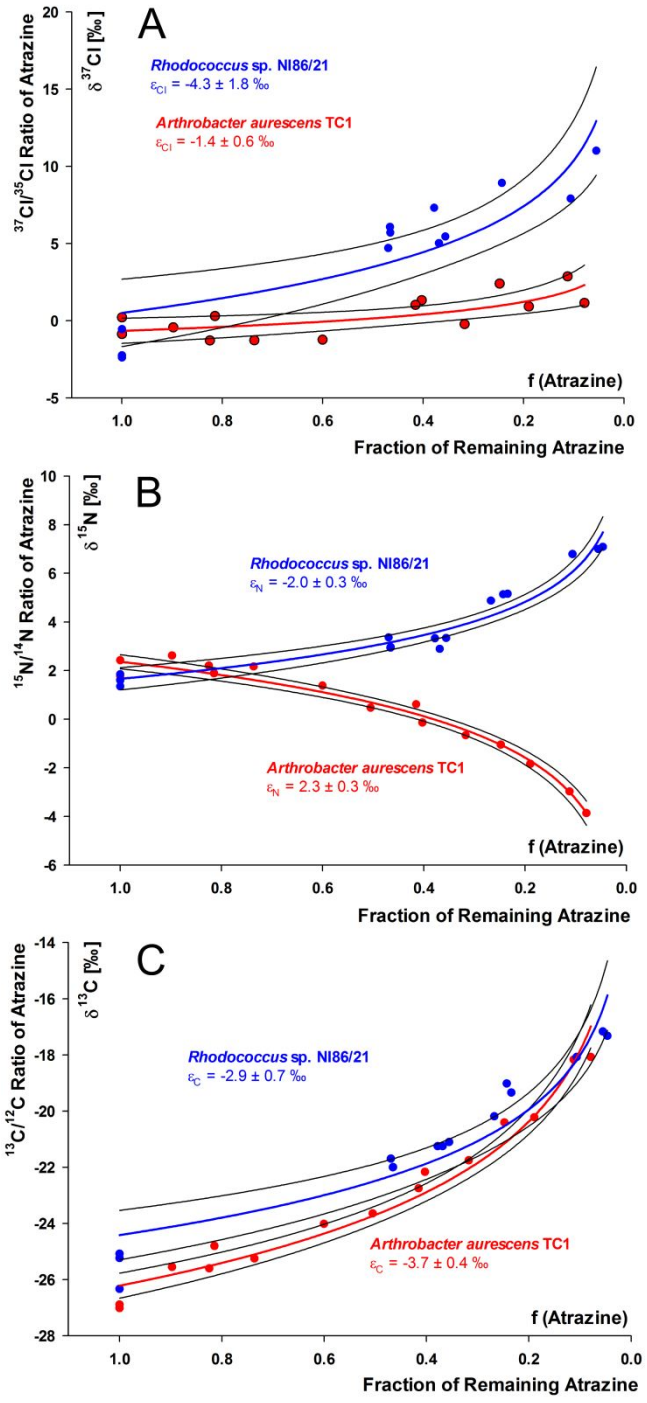

278

279 **Figure 2.** Isotope fractionation of (A) chlorine, (B) nitrogen and (C) carbon during

280 microbial degradation of atrazine by *A. aurescens* TC1 (red) and *Rhodococcus* sp.

NI86/21 (blue) and corresponding enrichment factors ε evaluated according to eq. 3. (The 95 % confidence intervals are given as values and as black lines).

Observed carbon and nitrogen isotope fractionation is consistent with previous studies. Carbon and nitrogen isotope fractionation for atrazine degradation by *A. aurescens* TC1 and *Rhodococcus* sp. NI86/21 was consistent with previous studies: Both experiments showed significant changes in isotope ratios (see Figure 2B and C). For hydrolysis with *A. aurescens* TC1, an inverse nitrogen isotope effect (ε_N = 2.3 ± 0.3 ‰) and a normal carbon isotope effect (ε_C = -3.7 ± 0.4 ‰) were observed, which were slightly smaller compared to the results of a former publication of Meyer et al. (ε_N = 3.3 ± 0.4 ‰, ε_C = -5.4 ± 0.6 ‰)[9], but gave the same dual element isotope plot ($\Lambda^{Arthro}_{C/N}$ = -0.6 ± 0.1) confirming that the same mechanism was at work (see Figure 3A).

Oxidative dealkylation of atrazine with *Rhodococcus* sp. NI86/21 resulted in a normal nitrogen isotope effect of ε_N = -2.0 ± 0.3 ‰ and a normal carbon isotope effect of ε_C = -2.9 ± 0.7 ‰. These ε-values are similar to those published by Meyer & Elsner[10] (ε_N = -1.5 ± 0.3 ‰, ε_C = -4.0 ± 0.2 ‰) and Meyer et al.[16] (ε_N = -1.4 ± 0.3 ‰, ε_C = -3.8 ± 0.2 ‰). The slightly more pronounced nitrogen isotope fractionation in this study can probably be attributed to the fact that oxidation was primarily observed at the C-H bond adjacent to the nitrogen atom (α-position of the ethyl or isopropyl group, see closed mass balance in Figure S5 in the SI)[16]. In the study of Meyer et al.[16] 48 % of the oxidation was observed at the β-position of the ethyl or isopropyl group resulting in a smaller nitrogen isotope

fractionation effect. The obtained regression slope of $\Lambda^{Rhodo}_{C/N}$ = 0.7 ± 0.1 in this study is slightly larger than the previously reported regression slopes ($\Lambda^{Rhodo}_{C/N}$ = 0.4 ± 0.1)[10, 16] which may again be explained by the small difference in average nitrogen isotope effects. Also here, however, the similar dual element isotope trend confirms that in this study atrazine was transformed by the same mechanism as in Meyer et al.[16] leading to the observed oxidative dealkylation products by *Rhodococcus* sp. NI86/21.

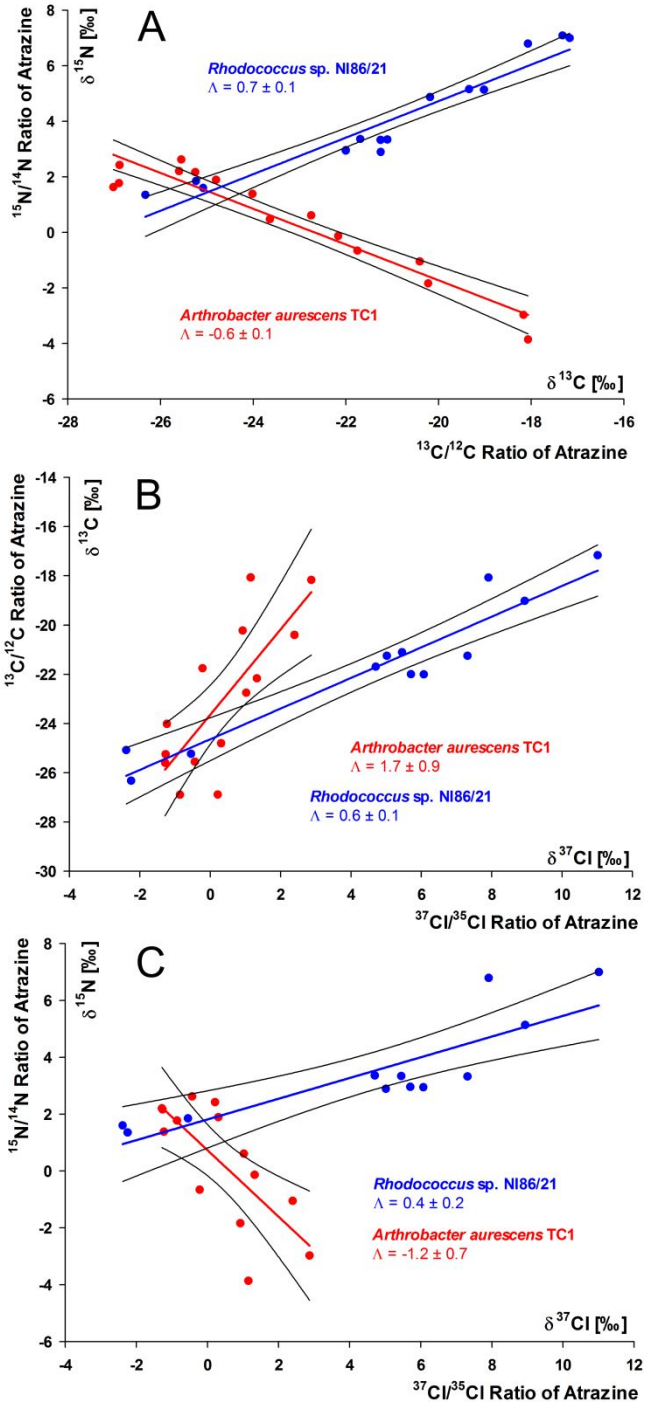

307

308 **Figure 3.** Isotope effects in microbial degradation of atrazine by *A. aurescens* TC1 (red)

309 and *Rhodococcus* sp. NI86/21 (blue) resulting in dual element isotope plots. (The 95 %

310 confidence intervals are given as values and as black lines next to the regression slopes).

311 (A) Regression slopes of nitrogen and carbon isotope values ($\Lambda_{C/N}$). (B) Regression
312 slopes of chlorine and carbon isotope values ($\Lambda_{Cl/C}$). (C) Regression slopes of chlorine
313 and nitrogen isotope values ($\Lambda_{Cl/N}$).

314 **Multi-element isotope approach.** Results of chlorine isotope analysis were combined
315 with data for carbon and nitrogen isotope measurements in dual element isotope plots
316 (see Figure 3B and C). For hydrolysis with *A. aurescens* TC1 regression slopes of
317 $\Lambda^{Arthro}_{Cl/C} = 1.7 \pm 0.9$ and $\Lambda^{Arthro}_{Cl/N} = -1.2 \pm 0.7$ were obtained. Oxidative dealkylation by
318 *Rhodococcus* sp. NI86/21 resulted in regression slopes of $\Lambda^{Rhodo}_{Cl/C} = 0.6 \pm 0.1$ and
319 $\Lambda^{Rhodo}_{Cl/N} = 0.4 \pm 0.2$. Since the dual element isotope plots of chlorine and carbon and of
320 chlorine and nitrogen provide significantly different regression slopes for the respective
321 elements, they can provide an additional line of evidence to differentiate the two
322 degradation mechanisms of atrazine from each other.

323 **Surprising mechanistic evidence from chlorine isotope effects.** For degradation with
324 *A. aurescens* TC1, rather small chlorine isotope fractionation was observed ($\varepsilon_{Cl} = -1.4$
325 $\pm$ 0.6 ‰) despite the fact that the chlorine is cleaved off during hydrolysis (see Figure 1).
326 For oxidative dealkylation with *Rhodococcus* sp. NI86/21, the chlorine is not cleaved off
327 (see Figure 1), therefore, no or just a small chlorine isotope effect was expected.
328 However, here more pronounced chlorine isotope fractionation was observed ($\varepsilon_{Cl} = -4.3$
329 $\pm$ 1.8 ‰).

330 The corresponding apparent kinetic isotope effects ($AKIE_{Cl,}$ see Table 1) were
331 compared to the $AKIE_{Cl}$ values of other studies focusing on the same degradation
332 mechanisms. In addition, the $AKIE_{Cl}$ values were compared to the theoretical maximum
333 Streitwieser Limit associated with the cleavage of a C-Cl bond (KIE_{Cl} = 1.02)[41-43] and to
334 the predictions of computational calculations (Table 2).

335 **Table 1.** $AKIE_{Cl}$ values associated with atrazine degradation.

Mechanism	$AKIE_{Cl}$	Study
Experimental Data		
abiotic alkaline hydrolysis (21 °C)	1.0069 ± 0.0005	Dybala-Defratyka et al.[35]
abiotic alkaline hydrolysis (50 °C),	1.0009 ± 0.0006	Grzybkowska et al.[36]
microbial hydrolysis (*A. aurescens* TC1)	1.0014 ± 0.0006*	this study
microbial dealkylation (*Rhodococcus* sp. NI86/21)	1.0043 ± 0.0018*	this study
Computational Data		
abiotic acidic/enzymatic hydrolysis (transition state 1)	range of 1.0002 to 1.0011	Grzybkowska et al.[36]
abiotic acidic/enzymatic hydrolysis (transition state 2)	1.0099	this study
abiotic neutral hydrolysis	1.0045	this study
abiotic alkaline hydrolysis	range of 1.0003 to 1.0014	Grzybkowska et al.[36]
enzymatic hydrolysis	range of 0.9996 to 1.0003	Szatkowski et al.[44]
abiotic dealkylation (hydrogen atom transfer by MnO_4^-)	0.9999	this study
abiotic dealkylation (hydride transfer by H_3O^+)	0.9997	this study

* calculated according to eq. 5

336

For microbial hydrolysis of atrazine an experimental $AKIE^{Arthro}_{Cl}$ value of 1.0014 ± 0.0006 was calculated (see Table 1). Dybala-Defratyka et al.[35] reported a more pronounced $AKIE^{alk.hydrol.}_{Cl}$ value of 1.0069 ± 0.0005 (see Table 1). However, that study[35] was conducted in an abiotic alkaline solution at 21 °C so that another hydrolysis pathway was involved. Newer data reported a much smaller value of $AKIE^{alk.hydrol.}_{Cl}$ = 1.0009 ± 0.0006[36] for the same alkaline hydrolysis at 50 °C. Later on it was confirmed that abiotic alkaline hydrolysis performed earlier at 21 °C resembles rather neutral than alkaline conditions[36]. Table 2 illustrates the different computed mechanisms that lie at the heart of the computational predictions. It shows the different mechanistic routes between the alkaline (substitution of Cl without protonation of the atrazine ring) and the acidic/enzymatic pathway characterized in Meyer et al.[9] (substitution of Cl with protonation of the atrazine ring) include different possible transition states. Chlorine KIEs are, among other factors[45], determined by the percent extension of the C-Cl bond in the transition state. As this is directly related to the structure of the transition state, it can be linked to the C-Cl bond orders (Table 2), which decrease in the studied hydrolysis reactions when the C-Cl bond is more ruptured as compared to its length in the reactants, resulting in increased chlorine KIEs. Previously performed computations[36] and computations of this study mimicking alkaline, acidic, and neutral conditions indicated that the largest $AKIE_{Cl}$ should be expected under neutral conditions (except for transition state 2 of acidic/enzymatic hydrolysis). Under neutral conditions the C-Cl bond is elongated leading to a transition state geometry which differs substantially from hydrolysis reactions promoted either by

358 alkaline or acidic conditions (see Table 2). However, hydrolysis at neutral pH is too slow
359 to be of relevance. Computational calculations taking into account the transition state
360 structures at a molecular level predicted $AKIE_{Cl}$ values ranging from 0.9996 to 1.0014 for
361 alkaline, acidic and enzymatic hydrolysis (see Table 1 and 2)[36, 44]. Hence, on the
362 mechanistic level, the computational studies predict that the formation of a Meisenheimer
363 complex rather than the subsequent C-Cl bond cleavage is the rate-determining step
364 during the nucleophilic aromatic substitution reaction catalyzed by TrzN[36, 44]. In both
365 abiotic pathways the C-Cl bond at the transition state of the rate determining step is
366 almost intact giving rise to very small $AKIE_{Cl}$ (the computed bond orders for both alkaline
367 and acidic hydrolysis are the same and equal to 1.03, see also Table 2). In this study, we
368 therefore observed a similarly small $AKIE^{Arthro}_{Cl}$ value for enzymatic hydrolysis in
369 *A. aurescens* TC1 which resembles acid-catalyzed hydrolysis rather than alkaline
370 hydrolysis[9]. Hence, the picture emerges that different hydrolytic pathways give rise to
371 experimental $AKIE_{Cl}$ values much lower than the Streitwieser Limit of 1.02[41-43] indicating
372 that the chlorine isotope effect is masked in all cases and that the C-Cl bond cleavage is
373 not the rate-determining step. Interestingly, this is in contrast to ametryn hydrolysis where
374 strong sulphur isotope effects were observed in enzymatic hydrolysis by TrzN[17]. Further
375 experimental work, including degradation experiments with other strains, hydrolysis and
376 crude enzyme experiments, will be required to further substantiate the picture on chlorine
377 isotope effects observed in this study. For the moment, since chlorine isotope effects were
378 found to be masked, we must conclude, however, that information from chlorine isotope

379 analysis alone would not be enough to differentiate the different reaction mechanisms.
380 This illustrates the importance of analyzing more than one element for mechanistic
381 differentiation.

382

383 **Table 2.** Mechanisms and transition states of acidic/enzymatic, neutral and alkaline hydrolysis and corresponding

384 calculated and measured isotope effects.

Mechanism	Calculated Transition State[a]	Calculated Isotope Effect (position-specific and compound average AKIE values)	Measured Isotope Effect
Acidic/Enzymatic Hydrolysis (Transition State 1) 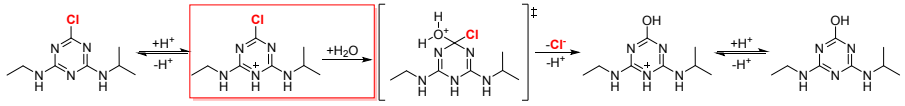	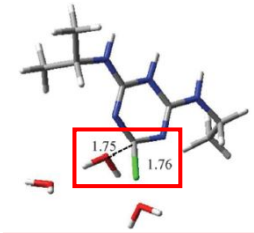 C-Cl Bond Order: 1.03	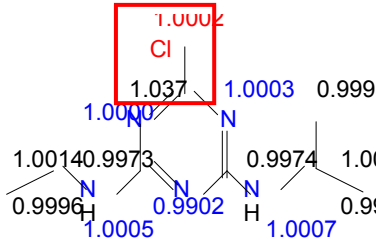 Compound average: $AKIE_{Cl}$ = 1.0002[a] $AKIE_N$ = 0.9983[a] $AKIE_C$ = 1.0042[a]	Compound average: ~~$AKIE_{Cl}$ = 1.0014 ± 0.0006[b]~~ $AKIE_N$ = 0.9886 ± 0.0015[b] $AKIE_C$ =1.0271 ± 0.0034[b]
Acidic/Enzymatic Hydrolysis (Transition State 2) 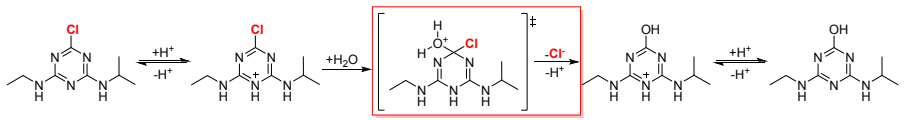	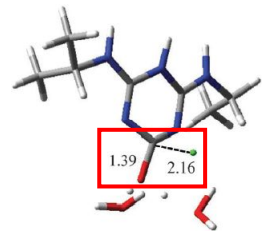 C-Cl Bond Order: 0.55	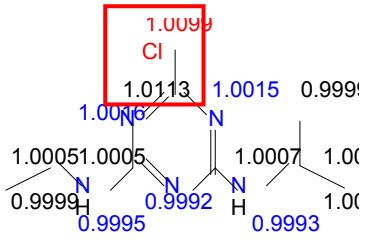 Compound average: $AKIE_{Cl}$ = 1.0099 $AKIE_N$ = 1.0002 $AKIE_C$ = 1.0017	-
Neutral Hydrolysis 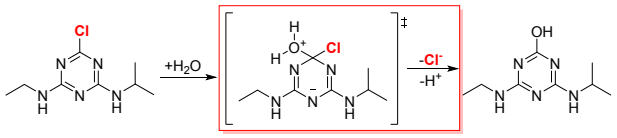	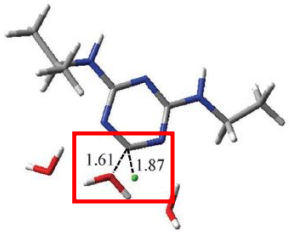 C-Cl Bond Order: 0.87	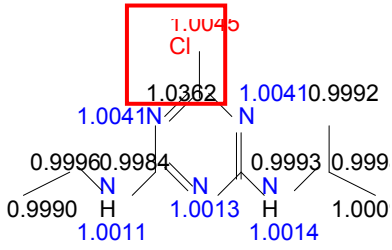 Compound average: $AKIE_{Cl}$ = 1.0045 $AKIE_N$ = 1.0024 $AKIE_C$ = 1.0041	-

Alkaline Hydrolyis			
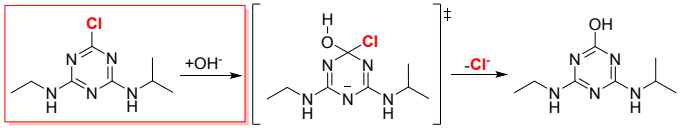	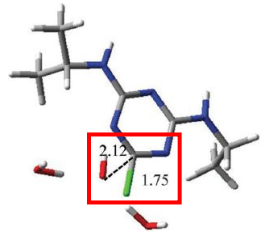 C-Cl Bond Order: 1.03	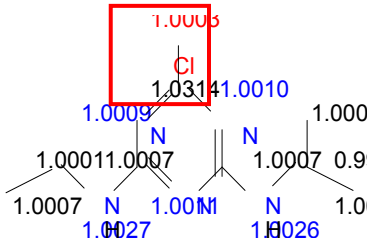	Compound average: $AKIE_{Cl}$ = 1.0003[a] $AKIE_N$ = 1.0017[a] $AKIE_C$ =1.0043[a]

Compound average:
~~$AKIE_{Cl}$ = 1.0009 ± 0.0006[a]~~
$AKIE_N$ = 1.001 ± 0.000[c]
$AKIE_C$ =1.031 ± 0.003[c]

385 [a] taken from Grzybkowska et al.[36], [b] calculated according to eq. 5 with n = 5 for N and n = 8 for C, [c] taken from Meyer et al.[9]

386

For oxidative dealkylation, so far, no chlorine isotope effects were reported. Regarding the reaction mechanism, Meyer et al.[16] concluded that oxidative dealkylation of atrazine with *Rhodococcus* sp. NI86/21 is initiated by hydrogen atom transfer based on the observed product distribution and the carbon and nitrogen isotope effects. Hydrogen atom transfer leads directly to a homolytic cleavage of the C-H bond adjacent to the nitrogen atom (α-position of the ethyl or isopropyl group) producing a relative unstable 1,1-aminoalcohol which is then further transformed to DEA or DIA[16]. In parallel, two additional products could be detected which were formed by oxidation of the C-H bond in the β-position of the ethyl or isopropyl group. For this mechanistic pathway, chlorine isotope effects would be expected to be rather small since the chlorine is not involved in the reaction steps. The closed mass balance of the concentration analysis (see Figure S5 in the SI) of this study and the results of product distribution of Meyer et al.[16] also indicate that there is no C-Cl bond cleavage taking place since corresponding hydrolysis products were not detected. Furthermore, our computations for hydrogen atom transfer at a catalytic center mimicking cytochrome P450 predicted no chlorine isotope effect ($AKIE^{hydro.atom\ trans.}_{Cl}$ = 0.9999, see Table 1). Hydride transfer promoted by the hydronium ion also resulted in no chlorine isotope effect ($AKIE^{hydride\ trans.}_{Cl}$ = 0.9997, see Table 1). At previously located transition state structures for these two reactions[16] the carbon-chlorine bond remains intact and no stretching of this bond is involved in the reaction coordinate (hydrogen transfer) mode. The observed more pronounced $AKIE^{Rhodo}_{Cl}$ value of 1.0043 ±0.0018 in this study (see Table 1) could, therefore, be indicative of isotope effects

caused by enzymatic interactions. Meyer et al.[16] proposed that for oxidative dealkylation no selectivity itself is observed, however, the preferred oxidation of the α-position over the β-position could be explained by steric factors of the catalyzing enzyme which could have an influence on the transformation pathway. Thus, the sensitive chlorine isotope effect, which is observed even though the C-Cl bond is not cleaved during degradation, can be interpreted as an indicator that non-covalent interactions between the cytochrome P450 complex and the chlorine cause significant chlorine isotope fractionation[46].

CONCLUSION

Since atrazine is frequently detected in groundwater systems, major efforts should be put into understanding its environmental fate. We provide an approach to 3D-isotope (C, N, Cl) analysis of atrazine and explored isotope fractionation in different transformation pathways. Together, this provides the basis to more confidently assess sources and degradation of atrazine in the environment. Specifically, we demonstrated that pronounced changes in chlorine isotope values are not an indicator of microbial hydrolysis (as one might have expected without knowledge of our experimental data), but – surprisingly – rather of oxidative dealkylation. Therefore, although trends are different than expected, they can nonetheless be used for a more confident identification of different sources and transformation pathways in field samples. Regarding the sensitivity of chlorine isotope effects, our study demonstrates the importance of performing

controlled laboratory experiments before applying the approach in the field. Specifically, in other cases chlorine isotope fractionation can be much more pronounced than observed for atrazine in this study. Large chlorine isotope effects were observed in proof-of-principle experiments by Ponsin et al.[20] studying hydrolytic dechlorination of S-metolachlor, an herbicide containing also only one chlorine atom. Here preliminary data suggest a large chlorine isotope effect of ε_{Cl} = -9.7 ± 2.9 ‰ for abiotic alkaline hydrolysis. Therefore, in the case of other substances chlorine isotope effects can be even more sensitive indicators of degradation provided that the C-Cl bond cleavage occurs in the rate-determining step of a reaction. Further, gaining deeper insights into these chemical processes is the basis for understanding the biotic catalysis of organic micropollutant degradation. This, in turn, is essential for identifying and developing optimized strategies for micropollutant removal in order to make successful bioremediation possible.

CONFLICT OF INTEREST

There are no conflicts to declare.

ACKNOWLEDGMENT

This work was supported by the Swiss National Science Foundation (SNSF, Grant CRSII2_141805), the German Israeli Foundation for Scientific Research and Development (GIF, Grant I-251-307.4-2013) and the National Science Center in Poland (Sonata BIS grant UMO-2014/14/E/ST4/00041). We thank PLGrid Infrastructure

(Poland) for computer resources and Armin Meyer for his advice regarding the microbial degradation experiments.

REFERENCES

1. H. Gysin and E. Knusli, Chemistry and herbicidal properties of triazine derivatives, *Adv. in Pest Control Res.*, 1960, **3**, 289-353.
2. EPA, Pesticides Industry Sales and Usage: 2008–2012 Market Estimates, *US Environmental Protection Agency, Washington (DC)*, 2017.
3. European Commission, Commission decision of 10 March 2004 concerning the non-inclusion of atrazine in Annex I to Council Directive 91/414/EEC and the withdrawal of authorisations for plant protection products containing this active substance., *Official Journal of the European Union*, 2004, **78**, 53-55.
4. R. Loos, G. Locoro, S. Comero, S. Contini, D. Schwesig, F. Werres, P. Balsaa, O. Gans, S. Weiss, L. Blaha, M. Bolchi and B. M. Gawlik, Pan-European survey on the occurrence of selected polar organic persistent pollutants in ground water, *Water Res.*, 2010, **44**, 4115-4126.
5. D. Vonberg, J. Vanderborght, N. Cremer, T. Pütz, M. Herbst and H. Vereecken, 20 years of long-term atrazine monitoring in a shallow aquifer in western Germany, *Water Res.*, 2014, **50**, 294-306.
6. S. Singh, V. Kumar, A. Chauhan, S. Datta, A. B. Wani, N. Singh and J. Singh, Toxicity, degradation and analysis of the herbicide atrazine, *Environ. Chem. Lett.*, 2018, **16**, 211-237.
7. S. Kern, H. P. Singer, J. Hollender, R. P. Schwarzenbach and K. Fenner, Assessing exposure to transformation products of soil-applied organic contaminants in surface water: comparison of model predictions and field data, *Environ. Sci. Technol.*, 2011, **45**, 2833-2841.
8. C. Moreau-Kervevan and C. Mouvet, Adsorption and desorption of atrazine, deethylatrazine, and hydroxyatrazine by soil components, *J. Environ. Qual.* , 1998, **27**, 46-53.

9. A. H. Meyer, H. Penning and M. Elsner, C and N isotope fractionation suggests similar mechanisms of microbial atrazine transformation despite involvement of different Enzymes (AtzA and TrzN), *Environ. Sci. Technol.*, 2009, **43**, 8079-8085.
10. A. H. Meyer and M. Elsner, 13C/12C and 15N/14N Isotope Analysis To Characterize Degradation of Atrazine: Evidence from Parent and Daughter Compound Values, *Environ. Sci. Technol.*, 2013, **47**, 6884-6891.
11. A. H. Meyer, H. Penning, H. Lowag and M. Elsner, Precise and accurate compound specific carbon and nitrogen isotope analysis of atrazine: critical role of combustion oven conditions, *Environ. Sci. Technol.*, 2008, **42**, 7757-7763.
12. S. Reinnicke, D. Juchelka, S. Steinbeiss, A. H. Meyer, A. Hilkert and M. Elsner, Gas chromatography-isotope ratio mass spectrometry (GC-IRMS) of recalcitrant target compounds: performance of different combustion reactors and strategies for standardization, *Rapid. Commun. Mass. Sp.*, 2012, **26**, 1053-1060.
13. K. Schreglmann, M. Hoeche, S. Steinbeiss, S. Reinnicke and M. Elsner, Carbon and nitrogen isotope analysis of atrazine and desethylatrazine at sub-microgram per liter concentrations in groundwater, *Anal. Bioanal. Chem.*, 2013, **405**, 2857-2867.
14. T. C. Schmidt, L. Zwank, M. Elsner, M. Berg, R. U. Meckenstock and S. B. Haderlein, Compound-specific stable isotope analysis of organic contaminants in natural environments: a critical review of the state of the art, prospects, and future challenges, *Anal. Bioanal. Chem.*, 2004, **378**, 283-300.
15. M. Elsner, Stable isotope fractionation to investigate natural transformation mechanisms of organic contaminants: principles, prospects and limitations, *J. Environ. Monit.*, 2010, **12**, 2005-2031.
16. A. H. Meyer, A. Dybala-Defratyka, P. J. Alaimo, I. Geronimo, A. D. Sanchez, C. J. Cramer and M. Elsner, Cytochrome P450-catalyzed dealklyation of atrazine by *Rhodococcus* sp. strain NI86/21 involves hydogen atom transfer rather than single electorn transfer, *Dalton Trans.*, 2014, **43**, 12111-12432.
17. H. K. V. Schürner, J. L. Seffernick, A. Grzybkowska, A. Dybala-Defratyka, L. P. Wackett and M. Elsner, Characteristic Isotope Fractionation Patterns in s-

505 Triazine Degradation Have Their Origin in Multiple Protonation Options in the s-
506 Triazine Hydrolase TrzN, *Environ. Sci. Technol.*, 2015, **49**, 3490-3498.
507 18. T. B. Hofstetter and M. Berg, Assessing transformation processes of organic
508 contaminants by compound-specific stable isotope analysis, *TrAC, Trends Anal.*
509 *Chem.*, 2011, **30**, 618-627.
510 19. J. Renpenning, A. Horst, M. Schmidt and M. Gehre, Online isotope analysis of
511 37Cl/35Cl universally applied for semi-volatile organic compounds using GC-MC-
512 ICPMS, *J. Anal. At. Spectrom.*, 2018, **33**, 314-321.
513 20. V. Ponsin, C. Torrentó, C. Lihl, M. Elsner and D. Hunkeler, Compound-specific
514 chlorine isotope analysis of the herbicides atrazine, acetochlor and metolachlor,
515 *Anal. Chem.*, 2019, **91**, 14290-14298.
516 21. C. Lihl, L. M. Douglas, S. Franke, A. Pérez-de-Mora, A. H. Meyer, M. Daubmeier,
517 E. A. Edwards, I. Nijenhuis, B. Sherwood Lollar and M. Elsner, Mechanistic
518 Dichotomy in Bacterial Trichloroethene Dechlorination Revealed by Carbon and
519 Chlorine Isotope Effects, *Environ. Sci. Technol.*, 2019, **53**, 4245-4254.
520 22. L. E. Erickson, Degradation of atrazine and related s-triazines, *Crit. Rev. Env.*
521 *Con.*, 1989, **19**, 1-14.
522 23. H. M. LeBaron, J. E. McFarland and O. C. Burnside, *The triazine herbicides*,
523 Elsevier, Oxford, 1 edn., 2008.
524 24. L. C. Strong, C. Rosendahl, G. Johnson, M. J. Sadowsky and L. P. Wackett,
525 *Arthrobacter aurescens* TC1 metabolizes diverse s-triazine ring compounds,
526 *Appl. Environ. Microbiol.*, 2002, **68**, 5973-5980.
527 25. K. Sajjaphan, N. Shapir, L. P. Wackett, M. Palmer, B. Blackmon, J. Tomkins and
528 M. J. Sadowsky, *Arthrobacter aurescens* TC1 Atrazine Catabolism Genes *trzN*,
529 *atzB*, and *atzC* Are Linked on a 160-Kilobase Region and Are Functional in
530 *Escherichia coli*, *Appl. Environ. Microbiol.*, 2004, **70**, 4402-4407.
531 26. I. Nagy, F. Compernolle, K. Ghys, J. Vanderleyden and R. De Mot, A single
532 cytochrome P-450 system is involved in degradation of the herbicides EPTC (S-
533 ethyl dipropylthiocarbamate) and atrazine by Rhodococcus sp. strain NI86/21,
534 *Appl. Environ. Microbiol.*, 1995, **61**, 2056-2060.

27. M. Elsner, L. Zwank, D. Hunkeler and R. P. Schwarzenbach, A new concept linking observable stable isotope fractionation to transformation pathways of organic pollutants, *Environ. Sci. Technol.*, 2005, **39**, 6896-6916.
28. L. Zwank, M. Berg, M. Elsner, T. C. Schmidt, R. P. Schwarzenbach and S. B. Haderlein, New evaluation scheme for two-dimensional isotope analysis to decipher biodegradation processes: application to groundwater contamination by MTBE, *Environ. Sci. Technol.*, 2005, **39**, 1018-1029.
29. S. Reinnicke, A. Simonsen, S. R. Sørensen, J. Aamand and M. Elsner, C and N Isotope Fractionation during Biodegradation of the Pesticide Metabolite 2,6-Dichlorobenzamide (BAM): Potential for Environmental Assessments, *Environ. Sci. Technol.*, 2012, **46**, 1447-1454.
30. T. Gilevska, M. Gehre and H. H. Richnow, Multidimensional isotope analysis of carbon, hydrogen and oxygen as tool for identification of the origin of ibuprofen, *J. Pharm. Biomed. Anal.*, 2015, **115**, 410-417.
31. J. Palau, O. Shouakar-Stash, S. Hatijah Mortan, R. Yu, M. Rosell, E. Marco-Urrea, D. L. Freedman, R. Aravena, A. Soler and D. Hunkeler, Hydrogen Isotope Fractionation during the Biodegradation of 1,2-Dichloroethane: Potential for Pathway Identification Using a Multi-element (C, Cl, and H) Isotope Approach, *Environ. Sci. Technol.*, 2017, **51**, 10526-10535.
32. S. Franke, C. Lihl, J. Renpenning, M. Elsner and I. Nijenhuis, Triple-element compound-specific stable isotope analysis of 1,2-dichloroethane for characterization of the underlying dehalogenation reaction in two Dehalococcoides mccartyi strains, *FEMS Microbiol. Ecol.*, 2017, **93**, fix137.
33. T. Kuder, B. M. van Breukelen, M. Vanderford and P. Philp, 3D-CSIA: Carbon, Chlorine, and Hydrogen Isotope Fractionation in Transformation of TCE to Ethene by a Dehalococcoides Culture, *Environ. Sci. Technol.*, 2013, **47**, 9668-9677.
34. B. Heckel, K. McNeill and M. Elsner, Chlorinated Ethene Reactivity with Vitamin B12 Is Governed by Cobalamin Chloroethylcarbanions as Crossroads of Competing Pathways, *ACS Catal.*, 2018, **8**, 3054-3066.

35. A. Dybala-Defratyka, L. Szatkowski, R. Kaminski, M. Wujec, A. Siwek and P. Paneth, Kinetic isotope effects on dehalogenations at an aromatic carbon, *Environ. Sci. Technol.*, 2008, **42**, 7744-7750.
36. A. Grzybkowska, R. Kaminski and A. Dybala-Defratyka, Theoretical predictions of isotope effects versus their experimental values for an example of uncatalyzed hydrolysis of atrazine, *Phys. Chem. Chem. Phys.*, 2014, **16**, 15164-15172.
37. C. Lihl, J. Renpenning, S. Kümmel, F. Gelman, H. K. V. Schürner, M. Daubmeier, B. Heckel, A. Melsbach, A. Bernstein, O. Shouakar-Stash, M. Gehre and M. Elsner, Toward Improved Accuracy in Chlorine Isotope Analysis: Synthesis Routes for In-House Standards and Characterization via Complementary Mass Spectrometry Methods, *Anal. Chem.*, 2019, **91**, 12290-12297.
38. D. Hunkeler, R. U. Meckenstock, B. Sherwood Lollar, T. Schmidt, J. Wilson, T. Schmidt and J. Wilson, *A Guide for Assessing Biodegradation and Source Identification of Organic Ground Water Contaminants using Compound Specific Isotope Analysis (CSIA)*, O. o. R. a. Development Report PA 600/R-08/148 | December 2008 | www.epa.gov/ada, US EPA, Oklahoma, USA, 2008.
39. J. Bigeleisen, The relative reaction velocities of isotopic molecules, *J. Chem. Phys.*, 1949, **17**, 675-679.
40. V. Anisimov and P. Paneth, ISOEFF98. A program for studies of isotope effects using Hessian modifications, *J. Math. Chem.*, 1999, **26**.
41. A. Streitwieser Jr, R. Jagow, R. Fahey and S. Suzuki, Kinetic isotope effects in the acetolyses of deuterated cyclopentyl tosylates1, 2, *J. Am. Chem. Soc.*, 1958, **80**, 2326-2332.
42. K. Świderek and P. Paneth, Extending limits of chlorine kinetic isotope effects, *J. Org. Chem.*, 2012, **77**, 5120-5124.
43. L. Szatkowski and A. Dybala-Defratyka, A computational study on enzymatically driven oxidative coupling of chlorophenols: An indirect dehalogenation reaction, *Chemosphere*, 2013, **91**, 258-264.
44. L. Szatkowski, R. N. Manna, A. Grzybkowska, R. Kamiński, A. Dybala-Defratyka and P. Paneth, in *Methods in enzymology*, Elsevier, 2017, vol. 596, pp. 179-215.

595 45. A. Dybala-Defratyka, M. Rostkowski, O. Matsson, K. C. Westaway and P.
596 Paneth, A New Interpretation of Chlorine Leaving Group Kinetic Isotope Effects;
597 A Theoretical Approach, *J. Org. Chem.*, 2004, **69**, 4900-4905.
598 46. A. Siwek, R. Omi, K. Hirotsu, K. Jitsumori, N. Esaki, T. Kurihara and P. Paneth,
599 Binding modes of DL-2-haloacid dehalogenase revealed by crystallography,
600 modeling and isotope effects studies, *Arch. Biochem. Biophys.*, 2013, **540**, 26-
601 32.

602